minerals

MDPI

Article

Anaerobic Bioreduction of Jarosites and Biofilm Formation by a Natural Microbial Consortium

Laura Castro *, M. Luisa Blázquez, Felisa González, Jesús A. Muñoz and Antonio Ballester

Department of Chemical and Materials Engineering, Complutense University of Madrid, Av. Complutense s/n, 28040 Madrid, Spain; mlblazquez@quim.ucm.es (M.L.B.); fgonzalezg@quim.ucm.es (F.G.); jamunoz@quim.ucm.es (J.A.M.); ambape@quim.ucm.es (A.B.)

* Correspondence: lcastror@ucm.es

Received: 14 November 2018; Accepted: 25 January 2019; Published: 29 January 2019

Abstract: Jarosite occurs naturally in acid sulphate soils and is a common feature of streams impacted by acid mine drainage (AMD). Biological reduction of iron-sulphate minerals, such as jarosite, has the potential to contribute to the natural attenuation of acid mine drainage sites. The reduction of different jarosites (including minerals containing precious and toxic metals) by a natural bacterial/microbial consortium was examined in this study. Jarosites was used as a sole terminal electron acceptor via the reductive dissolution of Fe(III) minerals. The production of Fe(II) and the presence of sulphate-reducing bacteria in the consortium lead to the precipitation of metal sulphides immobilizing toxic heavy metals. Microbial attachment and biofilm formation of minerals have a great impact on the production and transformation of minerals and can influence the mobility of metals. After the adaptation to different jarosites, a unique specie was found: *Desulfosporosinus orientis*. *Desulfosporosinus* species are sulphate-reducing bacteria and can be found in sulphate-rich heavy metal-polluted environments, such as acid mine/rock drainage sites, being responsible for the sulphides formation. *D. orientis* is an obligate anaerobic microorganism and is able to reduce Fe(III) *D. orientis* is an obligate anaerobic microorganism and is able to reduce Fe(III). Confocal laser scanning microscopy and fluorescent lectin-binding analyses (FLBA) were used to study the arrangement and composition of the exopolysaccharides/glycoconjugates in biofilms indicating the presence of mannose, glucose, and *N*-acetylglucosamine residues. This study provides insights to understand the processes leading to the mobility or retention of metals in mine waste and industrial landfill environments.

Keywords: natural consortium; microbial reduction; jarosites; CLSM; biofilm

1. Introduction

Microorganisms play an important role in the biogeochemical cycling of iron in a variety of environments, from anaerobic aquifers or mine impacted areas to the deep sea floor [1–3]. In addition, the most abundant Fe(III)-minerals in near-surface aquatic and terrestrial systems are relatively insoluble due to the circumneutral pH and the oxidizing environment. Some microorganisms are able to use Fe(III)-bearing minerals as an electron acceptor. The products of this reduction can have an impact on the mobilization or sequestration of organic and inorganic pollutants, as well as on the subsequent geochemical reactions in soil and sedimentary environments. Biotic Fe(III) reduction in natural environments is a complex process affected by factors, such as the crystalline structure of the mineral and the degree of iron content [3–5].

Iron can be found on Earth in ferric or ferrous iron- bearing minerals in the form of oxyhydroxide, carbonate, phosphate or silicate. Jarosite [$MFe_3(SO_4)_2(OH)_6$] (M = metal), an iron hydroxysulphate

mineral, is common in acid soils, in mine waste in sulphate rich consitions or as a product of iron precipitation in metallurgical processes. Heavy metals, such as silver, lead and thallium can be naturally incorporated into jarosite by substitution of a proton, and anions, such as chromate, arsenate and selenate by substitution for SO_4^{2-}. Among the minerals of the jarosite subgroup, only argentojarosite and plumbojarosite are of economic importance as mineral species. In hydrometallurgical leaching circuits that employ jarosite precipitation, and especially in those circuits in which high temperatures and pressures are used, much of the silver can be detected in the jarosite fraction [6]. The oldest documented exploitation of Ag-bearing jarosite was at Rio Tinto, Spain, where the massive pyritiferous sulphide deposits have been oxidized to a gossan with a jarositic accumulation near its base.

Some microorganisms, such as *Shewanella putrefaciens* [7–9] and *Geobacter metallireducens* [3], cause changes of the aqueous chemistry due to the microbial reduction of jarosite, the mobility of heavy metals in the jarosite and the differences in decomposition behaviour of the minerals. Also, sulphate-reducing bacteria can promote the reduction of Fe(III) and the formation of iron sulphides, in which heavy metals and radionuclides released from jarosite can be incorporated into sulphides again [10].

The microorganisms in biofilms live embedded in a self-produced matrix of hydrated extracellular polymeric substances (EPS) that consist mainly of polysaccharides, proteins, nucleic acids and lipids. EPS provide mechanical stability to biofilms, mediate adhesion to solid surfaces and form a cohesive network that interconnects and immobilizes the cells in the biofilm matrix [11]. In addition, bacteria in biofilms exhibit emergent properties, such as physical and social interactions, resource capture by biofilms, enhanced rate of gene exchange and enhanced resistance or tolerance to antimicrobial agents [12]. Biotechnological applications of biofilms in different fields include bioremediation and water treatment, biocatalysis and microbial fuel cell technology. On the other side, bacterial biofilms can be responsible for infections, corrosion or water contamination.

For applied purposes, the adequate formation of biofilms and control of EPS production, results in the improved efficiency of the process. EPS can vary greatly in composition and structure between biofilms depending on the type of microorganisms, shear forces, temperature and availability of nutrients [13–15].

This work examined the anaerobic reduction of Fe(III)-ores: A mixture of potassium and ammonium jarosites, synthetic silver jarosite and gossan ore from Rio Tinto (Spain), using a natural microbial consortium. The gossans from Rio Tinto are oxidized materials composed of ferric minerals and various jarosite species [16]. Previous studies revealed that the ore is mainly composed of goethite, hematite and solid solutions of beudantite-plumbojarosite-potassium jarosite. Silver appears as halide, sulphide, mercury/silver sulpho-halide and as dilute solid solution of argentojarosite in jarosite-beudantite phases [17]. The dissimilatory Fe(III) reduction of these minerals by a natural microbial consortium from a mine site was studied considering the Fe(II) contained in the aqueous phase and in the precipitates and the resulting biogenic precipitates were studied by X ray diffraction. In addition, confocal laser scanning microscopy (CLSM) was used to investigate the excretion of adhesive EPS during attachment of bacterial cells to surfaces in the reduction process by a selection of fluorescently labeled lectins. The biofilm study provides insights to understand the processes involved in the mobility or retention of metals in mine waste and industrial landfill environments, but also to take into account new characteristic features of biofilms, such as social cooperation, resource capture and enhanced survival of exposure to antimicrobials.

2. Materials and Methods

2.1. Bacterial Cultures and Nutrient Medium

The natural microbial consortium was collected from the edge of an open-pit lake surrounding an abandoned mine site named "Brunita" (formerly a source of Pb-Zn ores) near La Unión (Murcia, Spain) (Figure S1). The water pH was 3.0–3.5. Sediments (6 g ca.) were sampled with a box-corer at a

depth of 30 cm to 45 cm and immediately transferred to sterile plastic tubes containing deionized and deoxygenated water (20 mL).

The bacterial culture was grown in modified Postgate C medium supplemented with Fe(III) (60 mM) using soluble ferric citrate and minerals (ammonium and potassium jarosites, silver jarosite and gossan) to provide an electron acceptor [18]. The medium was composed of the following salts ($g \cdot L^{-1}$): KH_2PO_4, 0.5; NH_4Cl, 1; Na_2SO_4, 4.5; $CaCl_2 \cdot 2H_2O$, 0.06; $MgSO_4 \cdot 7H_2O$, 0.06; sodium lactate, 6; yeast extract, 1; and sodium citrate$\cdot 2H_2O$, 0.3. The pH was adjusted with a pHmeter Basic20 (Crison) to 7.0 ± 0.2 using 10 M NaOH. The medium in flasks was vigorously bubbled with N_2:CO_2 (80/20, v/v) for 10 min to strip dissolved oxygen. The flasks were capped with butyl rubber stoppers and sealed with aluminium crimps. A 10% inoculum of an active culture was used. Cells were anaerobically grown at 30 ± 2 °C under static conditions.

The natural consortium was characterized using a method based on PCR amplification and denaturing gradient gel electrophoresis (DGGE) and sequencing of 16S rRNA gene fragments from both bacteria and archaea. The genomic DNA was used as a target in the PCR to amplify the 16S rRNA gene using the bacterial universal primer set 358FGC–907R and for Archaea 344FGC–915R. The DGGE fingerprint study was developed at the Biotechnology Centre of the Universidad Católica del Norte (Antofagasta, Chile) following the procedure described by Demergasso [19].

2.2. Preparation of Minerals

A pure culture of *Sulfolobus metallicus* DSM-6482 was used to generate the ammonium and potassium jarosite. The microorganism was grown in Norris medium [20] supplemented with 50 mM Fe^{2+} containing ($g \cdot L^{-1}$): $MgSO_4 \cdot 7H_2O$, 0.5; $(NH_4)_2SO_4$, 0.4 and K_2HPO_4, 0.2. The pH was adjusted to 1.8 using 1 M H_2SO_4, and the bacterial culture was incubated at 250 rpm and 70 ± 3 °C. The resultant ammonium jarosites were washed with deionized water, filtered through 0.20 μm pore-size nylon filters and dried at room temperature.

Silver jarosite was chemically obtained using the method developed by May [21].

The gossan mineral was collected from the Rio Tinto mine (Spain) to be used in a cyanidation plant and supplied by Rio Tinto Minera S.A. Gossan composition: Fe, 28.9 %; SiO_2, 43.8%; Pb, 1.55%; As, 0.67 %; K, 0.07 %; S (excluding S in barite), 0.51%; Sb, 0.11%; Cu, 0.061%; Zn, 0.021; Hg, 14 $g \cdot L^{-1}$ Ag, 41 $g \cdot L^{-1}$; Au, 1.0 $g \cdot L^{-1}$. The crushed ore presented a size < 40 μm (mesh size).

2.3. Kinetic Tests

Fe(III) reduction was evaluated in vials containing 30 mL of Postgate C medium supplemented with different minerals. Vials were inoculated with a bacterial culture volume of 10%. Chemical controls prepared with cell-free culture medium were also measured. Inoculated vials and controls were incubated under anaerobic and static conditions, in the dark at 30 ± 2 °C. All data on the experiments are averages of two parallel flasks.

Inoculated vials and controls were monitored periodically. The concentration of Fe^{2+} and total iron were measured to check the bacterial growth. Fe^{2+} and Fe_{total} were measured for the same sample. Sampling was carried out with a deoxygenated with a sterile mixture of N_2/CO_2 (80/20, v/v) and sterile syringe. Liquid samples were withdrawn, and once removed, immediately transferred to the HCl extraction solution to prevent Fe(II) oxidation.

Samples were collected in two different ways to determine the speciation of iron in both the solid and liquid phases: Two replicates were withdrawn from the clarified supernatant solution of settlement vials and another two replicates from shaken vials.

The duplicates of the 0.5 mL samples were mixed with the extraction solution (0.5 mL HCl solution 50% v/v) and heated until complete dissolution of the solid phase. After that, 4.0 mL of deionized water was added to the mixture.

HCl-extractable Fe^{2+} was determined spectrophotometrically by the ferrozine method measuring the absorbance of the ferrozine-Fe(II) complex at 562 nm after 5 min of color development [22].

Standards of Fe(II) for the ferrozine assay were prepared with ferrous ethylene diammonium sulphate tetrahydrate dissolved in 0.5 N HCl [23]. HCl-extractable total iron was determined in the same diluted acidic solution by atomic absorption spectroscopy with a Perkin-Elmer HGA 700.

2.4. Ion Chromatography

Anion concentration (lactate, citrate and acetate) was measured by ion chromatography. Measurements were carried out with a chromatograph 881 Compact ICpro (Metrohm, Herisau, Switzerland) equipped with a suppressor and a conductivity detector Metrohm 850 Professional IC. The ion exchange column was composed of polyvinyl alcohols (Metrohm Metrosep A Supp 7–150/4.0). Samples were injected via a 20 µL loop (flow 0.7 mL/min).

The solution to regenerate the suppressor was 250 mM H_2SO_4. The eluent was a mixture of two solutions: 1 mM Na_2CO_3 and 15 mM Na_2CO_3 (proportions change during the experiments). Samples were diluted with deionized water 1:100 and filtered through 0.2 µm Millipore filters before injection in the equipment. Data were registered using the software Magicnet 3.2 (Metrohm).

2.5. X-ray Diffraction Analysis

The air-dried precipitates generated by the microorganisms were mineralogically characterized by X-ray diffraction. Powder X-ray diffraction (XRD, Malvern PANalytical, Almelo, The Netherlands) was performed on a Philips X'pert-MPD equipment with a Cu anode operating at a wavelength of 1.5406 Å as the radiance source. The scanning range was from 10° to 60° 2θ with an angular interval of 0.05° and 4 s counting time. The crystalline phases were identified using standard cards from the International Centre for Diffraction Data (ICDD, Newtown Square, PA, USA) Powder Diffraction File database.

2.6. Field Emission Scanning Electron Microscopy (FE-SEM)

Bacterial cultures grown on lactate/gossan medium were filtered onto a 0.2 µm pore-size nylon filters. The samples were successively dehydrated with acetone and stored overnight at 4 °C in 90% acetone. The samples were critical-point dried and coated with graphite and gold for 2 min and 40 s at a Quorum Q150R S equipment, Quorum Technologies Ltd, Laughton, UK.

The examination of solid phase specimens and the spatial distribution of bacteria on mineral were performed with a JEOL JSM-6330 F microscope (JEOL, Tokyo, Japan) at 5–20 kV.

2.7. Confocal Laser Scanning Microscopy (CLSM)

Confocal laser scanning microscopy (CLSM, Zeiss, Jena, Germany) is used for DNA and lectin binding assay. The observation of the fluorescent signals was carried out using a laser scanning module Zeiss LSM 510 coupled with an inverted microscope 100 M BP (Zeiss). The different signals corresponding to the respective laser wavelength were recorded separately in a multi-track. Images were analyzed with software programs LSM 510 version SP2 (Zeiss), Volocity 3.5 (Improvision) and AxioVersion 3.1 (Zeiss).

2.7.1. Nucleic Acid Staining

The cell biomass and spatial distribution were visualized after staining with the nucleic acid stains (Invitrogen): Diamidino-2-phenylindole (DAPI), SYTO 9 and SYTO 62. DAPI is a blue-fluorescent DNA stain that is able to bind to AT regions of dsDNA. SYTO 9 is a green fluorescent nucleic acid dye to stain live and dead Gram-positive and Gram-negative bacteria. The cell-permeant SYTO 62 is a red fluorescent nucleic acid stain. Nucleic acid staining was done by covering the samples with 6 µM Invitogen stains for 15 min. Then, the sample was washed once with basal salt solution (medium salts without carbon sources).

2.7.2. Lectin Binding Assays

Ten lectins (Invitrogen) were selected to determine whether the EPS contained terminal fucose, mannose, glucose, galactose, glucosamine, *N*-acetyl galactosamine or other residues. To label carbohydrates ten fluoresceine isothiocyanate (FITC) and tetramethylrhodamine isothiocyanate (TRITC) labeled lectins have been used and they are summarized in Table 1. Samples were incubated with 0.05 mg/mL lectins for 40 min at room temperature. In order to remove the non-bound lectins, samples were washed three times with filter-sterilized water. The procedure was carried out avoiding direct light exposure as much as possible. The fluorescence of the dyes was prolonged by using an antifading agent (Citifluor™AF2) when mounting the samples.

Table 1. Characteristics of lectins employed in this study.

Lectin	Origin	Label	Specificity
Concanavalin A (Con A)	*Canavalia ensiformis*	TRITC	α-mannose, α-glucose
Peanut agglutinin (PNA)	*Arachis hypogaea*	FITC	galactose, *N*-acetylgalactosamine
Lens culinaris hemagglutinin (LcH)	*Lens culinaris*	FITC	α-mannose
Wheat germ agglutinin (WGA)	*Triticum vulgaris*	FITC	*N*-acetylglucosamine
Erythrina cristagalli (ECA)	*Erythrina cristagalli*	FITC	β-galactose, *N*-acetylgalactosamine
Soybean agglutinin (SBA)	*Glycine max*	FITC	α- or β-*N*-acetylgalactosamine
Ulex europaeus agglutinin I (UEA I)	*Ulex europaeus*	FITC	α-1,2 fucose
Pokeweed mitogen (PWM)	*Phytolacca americana*	FITC	*N*-acetylglucosamine
Bandeiraea simplicifolia isolectin (BS I)	*Bandeiraea simplicifolia*	TRITC	α-D-galactosil or *N*-acetyl-α-D-galactosaminyl residues
Phaseolus vulgaris agglutinin E (PHAE)	*Phaseolus vulgaris*	FITC	Oligosaccharides

3. Results and Discussion

3.1. Growth of the Natural Consortium

An acidic abandoned mine site was sampled to isolate Fe(III)-reducing bacteria. Molecular analysis (DGGE) of the prokaryotic consortium revealed three different bands both in bacterial and in archaeal fingerprints (Figure S2). The culture analyzed by the molecular technique was adapted successively to grow under very restricted conditions and probably contained a reduced version of the originally present bacterial population (Table S1). The genus *Clostridium* was the most abundant. *Clostridium* species are flexible in the use of electron acceptors and are often dominant in enrichment cultures [24]. In addition, these bacteria have been used for attenuating heavy metal pollution by means of sulphide generation [25].

The metabolic respiration was followed by monitoring the generation of Fe(II) (Figure 1a). Abiotic control samples evidenced the absence of Fe(II) under the experimental conditions tested. Reduction of Fe (III)-citrate by the prokaryotic consortium was fast and effective: Complete Fe(III) bio-reduction was achieved within 36 h (Figure S3). However, Fe(II) did not remain in solution. As growth progressed, the concentration of Fe(II) in solution decreased, whereas the Fe(II) concentration measured in the acid extraction solution increased indicating the Fe(II) enrichment of the precipitate.

The concentration of the main anions (citrate, lactate and acetate) in the medium is shown in Figure 1b. The citrate was provided as Fe(III) compound and lactate were supplied as a carbon source; the acetate was a result of the microbial metabolism.

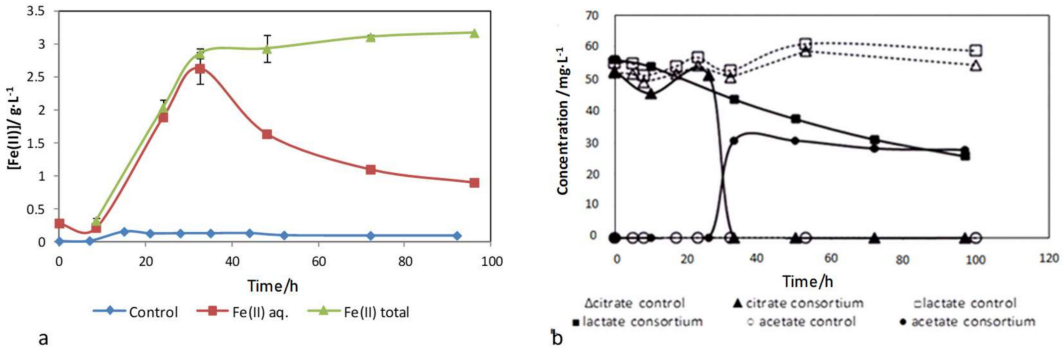

Figure 1. (**a**) Production of soluble and total Fe(II) by the natural consortium and (**b**) lactate, citrate and acetate concentrations in solution during the microbial reduction of ferric citrate provided as a sole iron source at 60 mM. All Fe(II) measurements were performed in duplicate by the ferrozine method and the standard deviation (n = 2) is shown for each data point. Error bars not visible are smaller than symbols.

The citrate concentration decreased sharply after 32 h, and simultaneously, acetate appeared in the medium and reached a concentration of 30 $mg \cdot L^{-1}$. Some microorganisms in the consortium used the citrate as a carbon source. The nature of the generated products depends on the pH of the medium [26]. At pH 7, formate and acetate are the main end products formed by the following reaction:

$$C_6H_5O_7{}^{-3} \rightarrow CO_2 + CHOO^- + 2CH_3COO^- \quad (1)$$

The degradation of citrate by fermentative bacteria causes the dissociation of Fe(III) ions from the Fe(III)-chelate and biogenic Fe(II) may precipitate as solid compounds. In addition, the lactate concentration decreased gradually, because some of the species present in the natural consortium are respiratory microorganisms. The products of the fermentative metabolism can be used by other species in the consortium as an electron source [27]. For instance, in sedimentary environments, in which Fe(III) reduction is the predominant terminal electron acceptor, the oxidation of organic matter takes place with the strong collaboration in a synergistic way between of fermentative and respiratory organisms.

Afterwards, the precipitate was recovered for analysis. X-ray analysis of the white precipitate recovered from the culture showed a Fe(II) compound: Siderite ($FeCO_3$). The CO_2 produced during the metabolism of organic compounds formed bicarbonate, which, in turn, promoted siderite formation:

$$CO_2 + H_2O \leftrightarrow H_2CO_3 \leftrightarrow H^+ + HCO_3{}^- \quad (2)$$

$$Fe^{2+} + HCO_3{}^- \rightarrow FeCO_3 + H^{+\cdot} \quad (3)$$

The chemical composition, relative abundance and distribution of the mineral and biogenic products are strongly influenced by the bacterial species involved in iron reduction [28].

3.2. Bioreduction of Minerals

This work was centered on the ability of a natural microbial consortium to reduce Fe(III)-bearing minerals, especially jarosites.

The change of color between the raw minerals and the residues generated in the inoculated vials evidenced the microbiological reduction of Fe(III). The color shifted from the original color: Yellow in

jarosites and orange in gossan, to black in the end-products produced by the microbial consortium, while the color of the control test remained unaltered.

The amount of biogenic Fe(II) was measured overtime evidencing the microbial growth (Figure 2). There was no significant accumulation of Fe(II) in the abiotic control samples. In contrast, the microbial culture was able to form Fe(II) from ferric minerals reduction under anaerobic conditions.

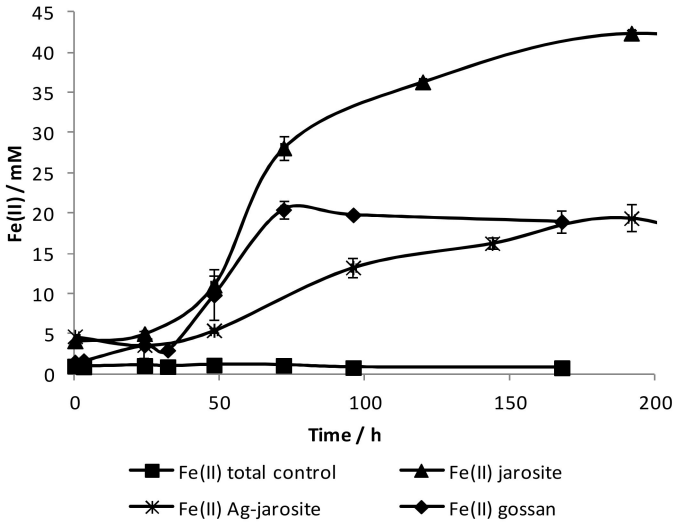

Figure 2. Fe(II) production by the natural consortium using different jarosite minerals as the sole iron source at 60 mM. All Fe(II) measurements were performed in duplicate by means of ferrozine method and standard deviation (n = 2) is shown for each data point. Error bars not visible are smaller than symbols.

Fe(III) bioreduction is strongly influenced by the chemical composition of the jarosites. The antibacterial properties of silver are well known [29]. The presence of this metal in Ag-jarosite may affect cell growth and biological mineral transformation. The maximum amount of Fe(II) produced by the natural consortium grown with ammonium and potassium jarosite was 42.4 ± 0.3 mM after 192 h.

Then, the consortium was grown with silver jarosite. After 192 h, the concentration of Fe(II) in the inoculated flasks was 19 ± 1 mM. The microbial Fe(III)-reduction rate and the formation of Fe(II) were much lower in case of silver jarosite than with ammonium and potassium jarosites. This behavior could be due to the toxicity of silver ions for some microorganisms in the consortium leading to the inhibition of the cell growth [9,30].

After this progressive adaptation to grow with different ferric minerals, the natural consortium was grown using a natural gossan ore from Rio Tinto, Spain. The maximum amount of Fe(II) was ~19.7 ± 0.7 mM after 72 h (3 days). The reaction speed was higher in comparison to the bioreduction of silver jarosite. Gossan mineral from Rio Tinto contains several heavy metals, such as Cu, Zn, Hg, Ag and Pb; however, these metals are not as concentrated as silver in silver jarosite. Nevertheless, microorganisms were not able to transform completely the gossan mineral.

The composition and the high crystallinity of the jarosites were confirmed by X ray diffraction analyses. This technique was also used to evidence changes in mineralogy after microbial mediated transformations in the inoculated samples (Figure 3). The precipitate produced by the prokaryotic consortium with potassium and ammonium jarosites showed a complex mixture of minerals and low crystallinity (Figure 3a). Apart from the unreacted jarosite, the compounds identified were siderite ($FeCO_3$), formed by the increased concentration of CO_2 due to the organic matter metabolism; and vivianite ($Fe_3(PO_4)_2 \cdot 8H_2O$), a ferrous phosphate precipitated by the bacteria [31]. Furthermore, the black colour of the precipitate observed after the reduction process is characteristic for FeS generated by sulphate-reducing bacteria. Sulphides were not detected by XRD studies probably due to its

amorphous nature. Nevertheless, the presence of FeS was evidenced when samples were dissolved in HCl and the characteristic H_2S odour was detected.

The precipitate produced by the prokaryotic microbial consortium with silver jarosite showed a complex mixture of minerals, including unreacted silver jarosite, siderite, vivianite, and silver compounds, such as silver sulphide (Figure 3b).

The analysis of X ray diffraction pattern of the raw gossan ore (Figure 3c) revealed that the main components in the mineral were quartz (SiO_2), goethite (FeO(OH)), hematite (Fe_2O_3), jarosites and silicates. The biogenic residues were identified as argentopyrite ($AgFe_2S_3$), where Fe(II), Fe(III) and Ag(I) appear co-precipitated, and siderite and vivianite as Fe(II)-containing minerals (Figure 3d). Furthermore, the goethite (ferric oxyhydroxide) appeared unreacted. It has been reported that the ability of microorganisms to reduce crystalline ferric minerals decreases following sequence lepidocrocite > goethite > hematite [4]. Hematite present in gossan mineral was transformed by the bacteria in the consortium; however, biogenic production of Fe(II) remained constant after 3 days of incubation and part of the other ferric phases contained in the gossan ore remain unreacted. A suitable explanation is that goethite was enclosed in the mineral matrix and cannot be reduced by the microorganisms.

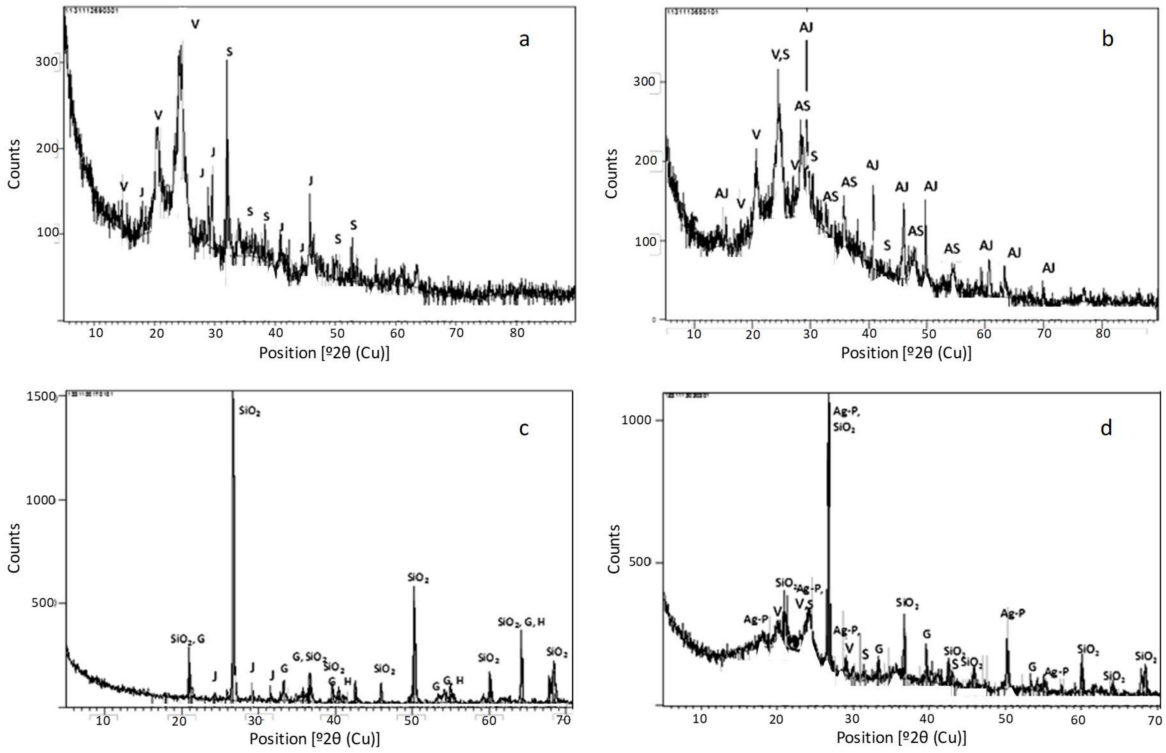

Figure 3. XRD patterns of the gossan mineral and the residues of different jarosites after microbial treatment: (**a**) Residue of K- and NH_4-jarosites (J = jarosite; S = siderite; V = vivianite); (**b**) residue of Ag-jarosite (AJ = argentojarosite; AS = silver sulphide; S = siderite; V = vivianite); (**c**) raw gossan mineral (G = goethite; H = hematite; SiO_2 = quartz; J = jarosite); and (**d**) residue of gossan mineral (Ag-S = argentopyrite; S = siderite; V = vivianite; G = goethite).

The jarositic mineral reduction was mediated by iron and/or sulphate-reducing bacteria. The presence of sulphate-reducing bacteria would be responsible for the formation of the black precipitate observed during the bioreduction process and identified by XRD as various metallic sulphides. These results highlight the suitability of jarosite to serve as a respiratory substrate for iron and sulphate-reducing bacteria.

$$2CH_3CHOHCOO^- + SO_4^{2-} \rightarrow 2CH_3COO^- + 2CO_2 + H_2S + 2OH^- \quad (4)$$

$$Me^{2+} + H_2S \rightarrow MeS\downarrow + 2H^+ \quad (5)$$

The residues from both tests, control and inoculated flasks, were observed by FE-SEM (Figures 4 and 5). The residues found in the microbial consortium microcosms contained a great number of transformed minerals indicating that Fe(III)-bearing solids had undergone changes in mineralogy by the action of microorganisms. These images provide evidence of a close association between microbes and solid surfaces. Changes in water chemistry (pH, Eh and composition) suggest that bacterial cells were using Fe(III) in the proximity of the mineral surface (Figure S3).

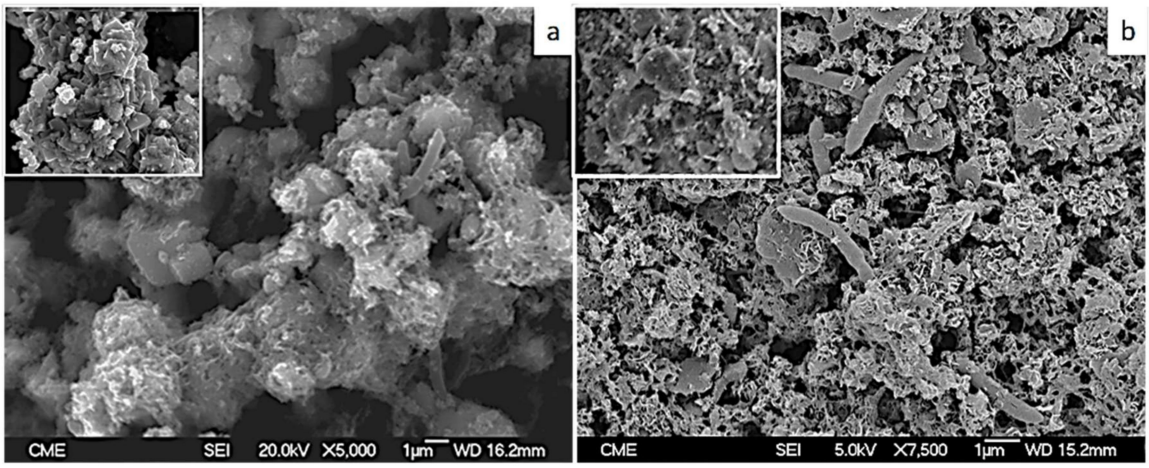

Figure 4. FE-SEM images of the mineral residues after incubation with microbes: (**a**) K- and NH_4-jarosites, and (**b**) gossan ore. Insets show the raw minerals.

The residues produced by microorganisms with silver jarosite were observed not only using secondary electrons, but also backscattered electrons microscopy (Figure 5). The brighter areas of the backscattered electron microscopy images, shown in Figure 6b, correspond to minerals, in which elements with a higher atomic number are concentrated (heavy metals). This image gives evidence of the presence of silver on the residue as silver sulphide, as identified by XRD analysis.

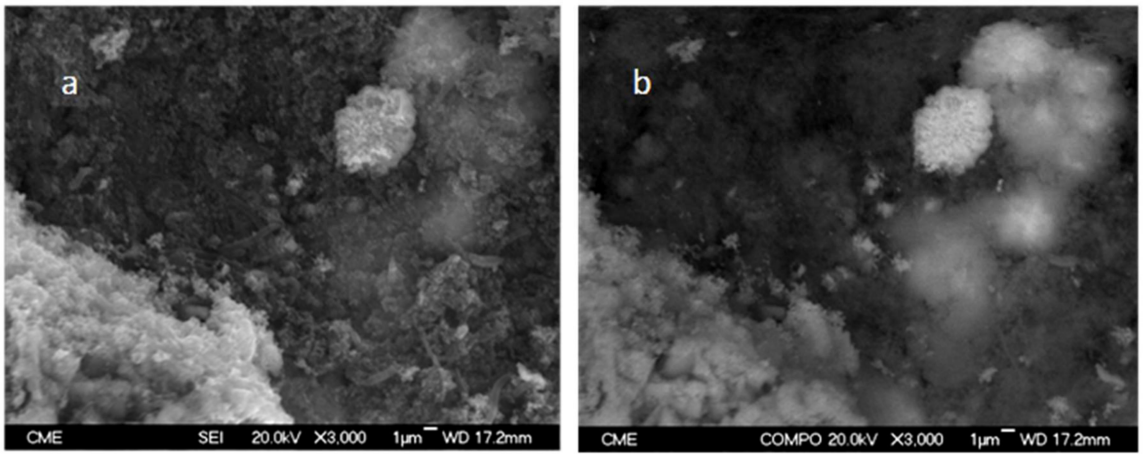

Figure 5. FE-SEM images of the residue of silver jarosite after incubation with microbes: (**a**) Secondary electrons, and (**b**) backscattered electrons.

After culturing the microorganisms with different jarosite compounds as an insoluble source of Fe(III), molecular analysis was carried out to observe the evolution of the natural consortium.

The analyses evidenced one band. The identification based on 16S rDNA sequencing showed 99% identity with *Desulfosporosinus orientis* DSM 765. *Desulfosporosinus* species are sulphate-reducing bacteria belonging to the *Firmicutes* and are mainly found in freshwater and water-saturated soils, but also in sulphate-rich heavy metal-polluted environments, such as acid mine/rock drainage sites [32]. *Desulfosporosinus* species are sulphate reducers for energy conservation, but some species can also grow by fermentative processes or using a variety of terminal electron acceptors, such as nitrate, Fe(III), or As(V). *D. orientis* is an obligate anaerobic microorganism and is able to reduce Fe(III) [33]. This specie uses a wide spectrum of energy sources, from aromatic compounds to short-chained fatty acids. *D. orientis* has been isolated from contaminated soils, and probably, its ability to reduce sulphate and precipitate metallic sulphides allowed the survival under these conditions.

The biodiversity in the consortium was remarkably reduced in comparison to the initial analysis. One explanation could be that the culture employed in the molecular analysis was successively adapted to grow under very restricted conditions using minerals containing high amounts of heavy metals, especially silver with its toxicity for many microorganisms.

3.3. Biofilm Formation

As it was previously shown, sulphate reducing bacteria can play beneficial roles in heavy metal and radionuclide bioremediation apart from their undesired participation in metal corrosion. Several studies with sulphate reducing bacteria biofilms have indicated that the reduction and precipitation of metal sulphides occur within the biofilm matrix [34]. Due to the applicability of these bacteria for bioremediation, biofilm research is needed to understand the cellular processes. Biofilms are formed by communities of microorganisms that are embedded in self-produced extracellular polymeric substances (EPS), which allow the attachment to different surfaces, such as mineral surfaces [35,36]. EPS are constituted by polysaccharides, protein, lipids and nucleic acids containing carboxyl, phosphoryl, amino, and hydroxyl on functional groups which can bind mineral surfaces. Confocal laser scanning microscopy (CLSM) is used to detect the formation of various EPS components within biofilms. This technique allows the identification of different EPS by the addition of specific fluorescent probes. Lectins are proteins or glycoproteins able to bind to specific residues in carbohydrates without modifying their structures.

Fluorescently labeled lectins in combination with other fluorochromes specific for nucleic acids provide a method to easily visualize glycoconjugate/biofilm on the mineral surface [37–39]. Analysis of biofilm composition using CLSM showed the diversity of chemical compounds present in a biofilm (Figure 6). A uniform distribution of the cells on the mineral surface was evidenced by the nucleic acid stain. Bacteria attached to the surface and developed a biofilm.

Four of the lectins tested were bound to the polysaccharides in the biofilm on the gossan mineral: ConA, Lens culinaris hemagglutinin (LcH), wheat germ agglutinin (WGA), and pokeweed mitogen (PWM). The combination of two stains (nucleic acids stains and lectins) applied sequentially to the same biofilm showing positive response is exhibited in Figure 6. Black areas in the images indicated where none of the stains were bound, and the presence of cells (blue for DAPI, green for SYTO 9 and red for SYTO 62), and lectins binding residues of cells or both.

Flocs in the culture were stained by Con A and lentil lectin; however, cells apparently were not stained. Living biofilms were stained by ConA and lentil lectin due to the presence of terminal mannosyl and terminal glucosyl residues in the polymeric compounds secreted by the microorganisms. Cellulose is commonly found in biofilm matrices, a linear polymer of (1-4)-β-linked glucose and in some strains appear to be necessary for biofilm formation [40]. *Pseudomonas aeruginosa* produces two polysaccharides: One named Psl, rich in mannose, which is necessary for the adhesion to the abiotic and biotic surface and in the stabilization of the biofilm structure [41], and the other called Pel, rich in glucose, has a key role in the formation of biofilms [42]. The staining of biofilms by WGA and PWM could be explained due to the specific binding to *N*-acetylglucosamine on the bacterial surface. In consequence, this amino sugar is probably involved in the biofilm formation and attachment to

mineral surfaces, but also in the intercellular adhesion. It is one of the most common polycationic exopolysaccharides in bacterial biofilms composed of β-1,6-linked *N*-acetylglucosamine with partly deacetylated residues and plays an important role in intercellular adhesion [43].

It has been also reported that sulphate reducing bacteria biofilms possess an abundance of proteins [44]. These bacteria are able to reduce metals and proteins could be involved as redox active molecules [45], facilitating and directing electron transfer, and support the efflux of heavy metals or toxic compounds present in potentially highly polluted water.

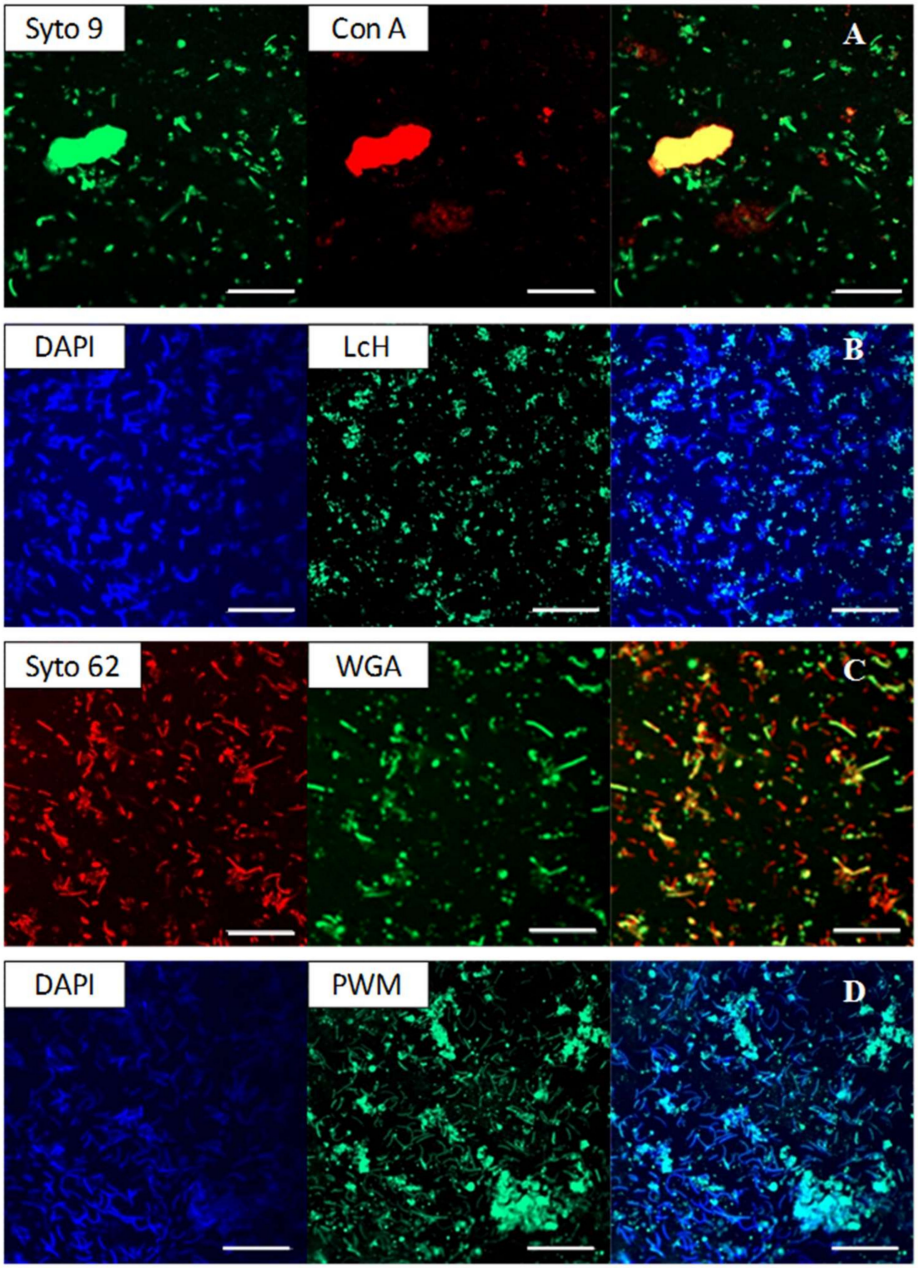

Figure 6. CLSM images of a biofilm region onto gossan mineral stained with different nucleic acid stains to show the distribution of bacterial cells within the biofilm. The region was also stained with several lectins: (**A**) Con A-TRITC, (**B**) LcH-FTIC, (**C**) WGA-FITC, and (**D**) PWM-FTIC. The last column shows the combination of the probes. Scale bars = 10 μm.

In many bacteria, exopolysaccharides play a key role in biofilm formation; however, mutants could not synthesize exopolysaccharides and became compromised or unable to form mature biofilms.

In mixed cultures, microbial species able to produce exopolysaccharides may facilitate the integration of other species unable to synthesize matrix polymers [42]. In consequence, extracellular polymeric substances serve as nutrients and are crucial in microbial ecology.

4. Conclusions

The natural consortium from an abandoned mine near La Unión reduced successfully Fe(III) ions from the ferric minerals forming a precipitate containing metal sulphides. Immobilization of toxic heavy metals in the residue is due to the presence of sulphate-reducing bacteria in the consortium responsible for the formation of metal sulphides. Consequently, this natural consortium could be applied in bioremediation both for mine environments and for the attenuation of acid mine drainage. Furthermore, the growth of the natural consortium in presence of different jarosites as Fe(III) source, some of them containing heavy metals with a hazardous effect, can reduce the biodiversity of the original culture. The molecular analysis after the bioreduction experiments indicated the presence of a unique specie: *Desulfosporosinus orientis*, a Gram-negative sulphate-reducing bacterium able to reduce Fe(III).

Fluorescently labelled lectin binding analysis provides evidence for the presence of mannose, glucose, and *N*-acetylglucosamine residues in the biofilm. Sulphate-reducing bacteria produce copious amounts of extracellular polymeric substances and the functional groups interact with the mineral surfaces and make cell adhesion and bioreduction possible.

Supplementary Materials: The following are available online at http://www.mdpi.com/2075-163X/9/2/81/s1, Figure S1: Geographic situation of the sampling site in the mining district of Cartagena-La Unión (Murcia, Spain). Corta Brunita ( ).; Figure S2: Stained denaturing gradient gel electrophoresis (DGGE) gels of bacterial and archaeal 16S rRNA gene fragments amplified by PCR. Numbered DGGE bands correspond to data presented in Table S1; Figure S3: pH and Eh variation during the bioreduction processes: (a) Soluble ferric citrate, (b) potassium and ammonium jarosites, (c) silver jarosite, and (d) gossan mineral; Table S1: DGGE results corresponding to the natural consortium grown on modified Postgate C medium with ferric citrate.

Author Contributions: Methodology and software, L.C.; validation, J.A.M., F.G. and A.B.; formal analysis, L.C.; investigation, L.C.; resources, J.A.M.; data curation, F.G. and L.C.; writing—original draft preparation, L.C.; writing—review and editing, J.A.M.; visualization, L.C. and A.B.; project administration, M.L.B.; funding acquisition, M.L.B.

Funding: The authors are grateful for the financial support given by the Spanish Ministry of Economy and Competitiveness to fund this work (project MAT2014-59222R).

Conflicts of Interest: The authors declare no conflict of interest.

References

1. Lovley, D.R. Dissimilatory Fe(III) and Mn(IV) reduction. *Microbiol. Rev.* **1991**, *55*, 259–287. [PubMed]
2. Wang, X.-J.; Yang, J.; Chen, X.-P.; Sun, G.-X.; Zhu, Y.-G. Phylogenetic diversity of dissimilatory ferric iron reducers in paddy soil of Hunan, South China. *J. Soil. Sediment.* **2009**, *9*, 568–577. [CrossRef]
3. Jones, E.J.P.; Nadeau, T.-L.; Voytek, M.A.; Landa, E.R. Role of microbial iron reduction in the dissolution of iron hydroxysulfate minerals. *J. Geophys. Res.* **2006**, *111*, G01012. [CrossRef]
4. Bonneville, S.; Behrends, T.; Van Cappellen, P. Solubility and dissimilatory reduction kinetics of iron(III) oxyhydroxides: A linear free energy relationship. *Geochim. Cosmochim. Ac.* **2009**, *73*, 5273–5282. [CrossRef]
5. Berthelin, J.; Ona-Nguema, G.; Stemmler, S.; Quantin, C.; Abdelmoula, M.; Jorand, F. Bioreduction of ferric species and biogenesis of green rusts in soils. *C. R. Geosci.* **2006**, *338*, 447–455. [CrossRef]
6. Dutrizac, J.E.; Jambor, J.L. Jarosites and their application in hydrometallurgy. *Rev. Mineral. Geochem.* **2000**, *40*, 405–452. [CrossRef]
7. Bingjie, O.; Xiancai, L.; Huan, L.; Juan, L.; Tingting, Z.; Xiangyu, Z.; Jianjun, L.; Rucheng, W. Reduction of jarosite by *Shewanella oneidensis* MR-1 and secondary mineralization. *Geochim. Cosmochim. Ac.* **2014**, *124*, 54–71. [CrossRef]
8. Smeaton, C.M.; Fryer, B.J.; Weisener, C.G. Intracellular precipitation of Pb by *Shewanella putrefaciens* CN32 during the reductive dissolution of Pb-jarosite. *Environ. Sci. Technol.* **2009**, *43*, 8086–8091. [CrossRef]
9. Weisener, C.G.; Babechuk, M.G.; Fryer, B.J.; Maunder, C. Microbial dissolution of silver jarosite: Examining its trace metal behaviour in reduced environments. *Geomicrobiol. J.* **2008**, *25*, 415–424. [CrossRef]

10. Li, Y.-L.; Vali, H.; Yang, J.; Phelps, T.J.; Zhang, C.L. Reduction of iron oxides enhanced by a sulfate-reducing bacterium and biogenic H_2S. *Geomicrobiol. J.* **2006**, *23*, 103–117. [CrossRef]
11. Sheng, G.-P.; Yu, H.-Q.; Li, X.-Y. Extracellular polymeric substances (EPS) of microbial aggregates in biological wastewater treatment systems: A review. *Biotechnol. Adv.* **2010**, *28*, 882–894. [CrossRef] [PubMed]
12. Flemming, H.-C.; Wingender, J.; Szewzyk, U.; Steinberg, P.; Rice, S.A.; Kjelleberg, S. Biofilms: An emergent form of bacterial life. *Nat. Rev. Microbiol.* **2016**, *14*, 563–575. [CrossRef] [PubMed]
13. Karunakaran, E.; Mukherjee, J.; Ramalingam, B.; Biggs, C. "Biofilmology": A multidisciplinary review of the study of microbial biofilms. *Appl. Microbiol. Biotechnol.* **2011**, *90*, 1869–1881. [CrossRef] [PubMed]
14. González, A.; Bellenberg, S.; Mamani, S.; Ruiz, L.; Echeverría, A.; Soulère, L.; Doutheau, A.; Demergasso, C.; Sand, W.; Queneau, Y.; et al. AHL signaling molecules with a large acyl chain enhance biofilm formation on sulfur and metal sulfides by the bioleaching bacterium *Acidithiobacillus ferrooxidans*. *Appl. Microbiol. Biotechnol.* **2013**, *97*, 3729–3737.
15. Bellenberg, S.; Leon-Morales, C.-F.; Sand, W.; Vera, M. Visualization of capsular polysaccharide induction in *Acidithiobacillus ferrooxidans*. *Hydrometallurgy* **2012**, *129–130*, 82–89. [CrossRef]
16. Sánchez, L.; Cruells, M.; Roca, A. Sulphidization-cyanidation of jarosite species: Applicability to the gossan ores of Rio Tinto. *Hydrometallurgy* **1996**, *42*, 35–49. [CrossRef]
17. Viñals, J.; Roca, A.; Cruells, M.; Núñez, C. Characterization and cyanidation of Rio Tinto gossan ores. *Can. Metall. Quart.* **1995**, *34*, 115–122. [CrossRef]
18. Castro, L.; García-Balboa, C.; González, F.; Ballester, A.; Blázquez, M.L.; Muñoz, J.A. Effectiveness of anaerobic iron bio-reduction of jarosite and the influence of humic substances. *Hydrometallurgy* **2013**, *131–132*, 29–33. [CrossRef]
19. Demergasso, C.S.; Galleguillos P, P.A.; Escudero G, L.V.; Zepeda A, V.J.; Castillo, D.; Casamayor, E.O. Molecular characterization of microbial populations in a low-grade copper ore bioleaching test heap. *Hydrometallurgy* **2005**, *80*, 241–253. [CrossRef]
20. Norris, P.R.; Barr, D.W. Growth and iron oxidation by acidophilic moderate thermophiles. *FEMS Microbiol. Lett.* **1985**, *28*, 221–224. [CrossRef]
21. May, A.; Sjoberg, J.J.; Baglin, E.G. Synthetic argentojarosite: Physical properties and thermal behavior. *Am. Mineral.* **1973**, *58*, 936–994.
22. Stookey, L. Ferrozine—A new spectrophotometric reagent for iron. *Anal. Chem.* **1970**, *42*, 779–781. [CrossRef]
23. Lee, J.-H.; Roh, Y.; Kim, K.-W.; Hur, H.-G. Organic acid-dependent iron mineral formation by a newly isolated iron-reducing bacterium, *Shewanella* sp. HN-41. *Geomicrobiol. J.* **2007**, *24*, 31–41. [CrossRef]
24. Coggon, M.; Becerra, C.A.; Nüsslein, K.; Miller, K.; Yuretich, R.; Ergas, S.J. Bioavailability of jarosite for stimulating acid mine drainage attenuation. *Geochim. Cosmochim. Ac.* **2012**, *78*, 65–76. [CrossRef]
25. Alexandrino, M.; Costa, R.; Canário, A.V.M.; Costa, M.C. Clostridia initiate heavy metal bioremoval in mixed sulfidogenic cultures. *Environ. Sci. Technol.* **2014**, *48*, 3378–3385. [CrossRef]
26. McFaddin, J.F. *Biochemical Tests for Identification of Medical Bacteria*; The Williams & Wilkins Company: Baltimore, MD, USA, 2000.
27. Scala, D.J.; Hacherl, E.L.; Cowan, R.; Young, L.Y.; Kosson, D.S. Characterization of Fe(III)-reducing enrichment cultures and isolation of Fe(III)-reducing bacteria from the Savannah River site, South Carolina. *Res. Microbiol.* **2006**, *157*, 772–783. [CrossRef] [PubMed]
28. Salas, E.C.; Berelson, W.M.; Hammond, D.E.; Kampf, A.R.; Nealson, K.H. The impact of bacterial strain on the products of dissimilatory iron reduction. *Geochim. Cosmochim. Ac.* **2010**, *74*, 574–583. [CrossRef]
29. Wakshlak, R.B.-K.; Pedahzur, R.; Avnir, D. Antibacterial activity of silver-killed bacteria: The "zombies" effect. *Sci. Rep. UK* **2015**, *5*, 9555. [CrossRef]
30. Adams, A.P.; Santschi, E.M.; Mellencamp, M.A. Antibacterial properties of a silver chloride-coated nylon wound dressing. *Vet. Surg.* **1999**, *28*, 219–225. [CrossRef]
31. Zachara, J.M.; Kukkadapu, R.K.; Fredrickson, J.K.; Gorby, Y.A.; Smith, S.C. Biomineralization of poorly crystalline Fe(III) oxides by dissimilatory metal reducing bacteria (DMRB). *Geomicrobiol. J.* **2002**, *19*, 179–207. [CrossRef]
32. Sanchez-Andrea, I.; Knittel, K.; Amann, R.; Amils, R.; Sanz, J.L. Quantification of Tinto River sediment microbial communities: Importance of sulfate-reducing bacteria and their role in attenuating acid mine drainage. *Appl. Environ. Microbiol.* **2012**, *78*, 4638–4645. [CrossRef]

33. Pester, M.; Brambilla, E.; Alazard, D.; Rattei, T.; Weinmaier, T.; Han, J.; Lucas, S.; Lapidus, A.; Cheng, J.F.; Goodwin, L.; et al. Complete genome sequences of *Desulfosporosinus orientis* DSM765T, *Desulfosporosinus youngiae* DSM17734T, *Desulfosporosinus meridiei* DSM13257T, and *Desulfosporosinus acidiphilus* DSM22704T. *J. Bacteriol.* **2012**, *194*, 6300–6301. [CrossRef] [PubMed]
34. Kiran, M.G.; Pakshirajan, K.; Das, G. Heavy metal removal from multicomponent system by sulfate reducing bacteria: Mechanism and cell surface characterization. *J. Hazard. Mater.* **2017**, *324*, 62–70. [CrossRef]
35. Gehrke, T.; Telegdi, J.; Thierry, D.; Sand, W. Importance of extracellular polymeric substances from *Thiobacillus ferrooxidans* for bioleaching. *Appl. Environ. Microbiol.* **1998**, *64*, 2743–2747. [PubMed]
36. Zhang, R.; Bellenberg, S.; Castro, L.; Neu, T.R.; Sand, W.; Vera, M. Colonization and biofilm formation of the extremely acidophilic archaeon *Ferroplasma acidiphilum*. *Hydrometallurgy* **2014**, *150*, 245–252. [CrossRef]
37. Zhang, R.Y.; Neu, T.R.; Bellenberg, S.; Kuhlicke, U.; Sand, W.; Vera, M. Use of lectins to in situ visualize glycoconjugates of extracellular polymeric substances in acidophilic archaeal biofilms. *Microb. Biotechnol.* **2015**, *8*, 448–461. [CrossRef]
38. Castro, L.; Zhang, R.; Muñoz, J.A.; González, F.; Blázquez, M.L.; Sand, W.; Ballester, A. Characterization of exopolymeric substances (EPS) produced by *Aeromonas hydrophila* under reducing conditions. *Biofouling* **2014**, *30*, 501–511. [CrossRef] [PubMed]
39. Zippel, B.; Neu, T.R. Characterization of glycoconjugates of extracellular polymeric substances in Tufa-associated biofilms by using fluorescence lectin-binding analysis. *Appl. Environ. Microbiol.* **2011**, *77*, 505–516. [CrossRef]
40. Karatan, E.; Watnick, P. Signals, regulatory networks, and materials that build and break bacterial biofilms. *Microbiol. Mol. Biol. R.* **2009**, *73*, 310–347. [CrossRef]
41. Colvin, K.M.; Irie, Y.; Tart, C.S.; Urbano, R.; Whitney, J.C.; Ryder, C.; Howell, P.L.; Wozniak, D.J.; Parsek, M.R. The Pel and Psl polysaccharides provide *Pseudomonas aeruginosa* structural redundancy within the biofilm matrix. *Environ. Microbiol.* **2012**, *14*, 1913–1928. [CrossRef]
42. Flemming, H.-C.; Wingender, J. The biofilm matrix. *Nat. Rev. Micro.* **2010**, *8*, 623–633. [CrossRef] [PubMed]
43. Izano, E.A.; Amarante, M.A.; Kher, W.B.; Kaplan, J.B. Differential roles of poly-N-acetylglucosamine surface polysaccharide and extracellular DNA in *Staphylococcus aureus* and *Staphylococcus epidermidis* biofilms. *Appl. Environ. Microbiol.* **2008**, *74*, 470–476. [CrossRef] [PubMed]
44. Clark, M.E.; Edelmann, R.E.; Duley, M.L.; Wall, J.D.; Fields, M.W. Biofilm formation in *Desulfovibrio vulgaris* Hildenborough is dependent upon protein filaments. *Environ. Microbiol.* **2007**, *9*, 2844–2854. [CrossRef] [PubMed]
45. Neu, T.R.; Lawrence, J.R. Chapter 37—Extracellular polymeric substances in microbial biofilms. In *Microbial Glycobiology*; Holst, O., Brennan, P.J., von Itzstein, M., Eds.; Academic Press: San Diego, CA, USA, 2010; pp. 733–758.